

Philip Desenfans

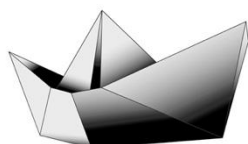
The Aerodynamics of a Falling Maple Seed

TYP DES DOKUMENTS | TYPE OF THE DOCUMENT

Studienarbeit | Study Thesis

Nachnutzung | Reuse

Diese Publikation steht unter der Creative-Commons-Lizenz Namensnennung - Nicht-kommerziell - Weitergabe unter gleichen Bedingungen 4.0 International (CC BY-NC-SA 4.0 International). Sofern der Name der Autor*innen/Rechteinhaber*innen genannt wird, kann der Inhalt vervielfältigt, verbreitet und öffentlich aufgeführt werden. Außerdem darf der Inhalt verändert werden (darunterfallen u. a. Übersetzungen des Werkes). Die Weitergabe der veränderten Fassung muss unter derselben Lizenz erfolgen. Der Inhalt darf nicht für kommerzielle Zwecke verwendet werden. Weitere Informationen und die vollständigen Bedingungen der Lizenz finden Sie hier: <https://creativecommons.org/licenses/by-nc-sa/4.0/legalcode>.



Project

The Aerodynamics of a Falling Maple Seed

Author: Philip Desenfans

Supervisor: Prof. Dr.-Ing. Dieter Scholz, MSME

Submitted: 2019-06-01

*Faculty of Engineering and Computer Science
Department of Automotive and Aeronautical Engineering*

DOI:

<https://doi.org/10.15488/9373>

URN:

<https://nbn-resolving.org/urn:nbn:de:gbv:18302-aero2019-06-01.016>

Associated URLs:

<https://nbn-resolving.org/html/urn:nbn:de:gbv:18302-aero2019-06-01.016>

© This work is protected by copyright

The work is licensed under a Creative Commons Attribution-NonCommercial-ShareAlike 4.0 International License: CC BY-NC-SA

<https://creativecommons.org/licenses/by-nc-sa/4.0>



Any further request may be directed to:

Prof. Dr.-Ing. Dieter Scholz, MSME

E-Mail see: <http://www.ProfScholz.de>

This work is part of:

Digital Library - Projects & Theses - Prof. Dr. Scholz

<http://library.ProfScholz.de>

Published by

Aircraft Design and Systems Group (AERO)

Department of Automotive and Aeronautical Engineering

Hamburg University of Applied Science

This report is deposited and archived:

- Deutsche Nationalbibliothek (<https://www.dnb.de>)
- Repositorium der Leibniz Universität Hannover (<https://www.repo.uni-hannover.de>)
- Internet Archive (<https://archive.org>), item: <https://archive.org/details/TextDesenfans.pdf>

Abstract

Purpose – The paper presents a theoretical framework that describes the aerodynamics of a falling maple (*Acer pseudoplatanus*) seed.

Methodology – A semi-empirical method is developed that provides a ratio stating how much longer a seed falls in air compared to freefall. The generated lift is calculated by evaluating the integral of two-dimensional airfoil elements using a preliminary falling speed. This allows for the calculation of the definitive falling speed using Blade Element Momentum Theory (BEMT); hereafter, the fall duration in air and in freefall are obtained. Furthermore, the input-variables of the calculation of lift are transformed to require only the length and width of the maple seed. Lastly, the method is applied to two calculation examples as a means of validation.

Findings –The two example calculations gave percentual errors of 5.5% and 3.7% for the falling speed when compared to measured values. The averaged result is that a maple seed falls 9.9 times longer in air when released from 20 m; however, this result is highly dependent on geometrical parameters which can be accounted for using the constructed method.

Research limitations – Firstly, the coefficient of lift is unknown for the shape of a maple seed. Secondly, the approximated transient state is yet to be verified by measurement.

Originality/ Value – The added value of this report lies in the reduction of simplifications compared to BEMT approaches. In this way a large amount of accuracy is achieved due to the inclusion of many geometrical parameters, even though simplicity is maintained. This has been accomplished through constructing a simple three-step method that is fundamental and essentially non-iterative.

The Aerodynamics of a Falling Maple Seed

Task for a project or thesis

Background

The maple seed (*Acer pseudoplatanus*) enters an autorotation after it is released from its stem, connecting it to the maple tree. During autorotation, the governing aerodynamics allow the seed to slow down its vertical velocity to a certain extent, rendering it more susceptible to effective wind dispersal. This evolutionarily shaped mechanism has pushed the aerodynamics of the winged seed towards very high efficiencies, constantly being put to the test in its race of survival. Subsequently, an understanding of these aerodynamical principles resulting in such high efficiencies would be truly valuable.

Task

Determine how much longer the seed falls using autorotational principles when compared to freefall. Examine this in constructing an aerodynamical framework following these steps:

- Start with a review to show what exists (or rather does not exist) on the topic.
- Calculate the lift generated by a maple seed and discuss the important derived equations.
- Use Blade Element Momentum Theory to calculate the equilibrium falling speed in air.
- Define a model that allows the calculation of a ratio declaring how much longer the seed falls in air.
- Validate the constructed method using calculation examples.
- Discuss your results and make recommendations.

The report has to be written in English based on German or international standards on report writing

Table of Contents

	Page
List of Figures	6
List of Tables	7
List of Symbols	9
List of Abbreviations.....	11
List of Definitions	12
1	
Introduction	14
1.1	14
Motivation	
1.2	15
Title Terminology.....	
1.3	15
Objectives	
1.4	16
Literature Review	
1.5	16
Structure.....	
2	
State of the Art	18
3	
Preliminary Equilibrium Falling Velocity	20
3.1	20
General Equation	
3.2	21
Inserting Parameter Values.....	
4	
Calculation of Lift	24
4.1	24
General Equation	
4.2	25
Deriving Chord Length.....	
4.3	28
Deriving Angle of Attack	
4.4	32
Deriving the Coefficient of Lift.....	
5	
Using BEMT to Calculate Falling Velocity	35
6	
Parametrization of Lift Formula	37
6.1	37
Parametrizing Chord Length	
6.2	38
Parametrizing Twist.....	
6.3	39
Parametrizing Total Surface Area and Tip Loss Correction	
7	
Calculation of Fallen Distance	40
7.1	40
Fallen Distance Including Aerodynamic Effects.....	
7.2	43
Fallen Distance in Freefall.....	
7.3	43
Falling Time Ratio.....	
8	
Calculation Examples	45
8.1	45
Example One	
8.1.1	45
Preliminary Falling Speed	
8.1.2	46
Calculation of Lift	
8.1.3	47
Calculation of Equilibrium Falling Speed	

8.1.4	Reiteration	48
8.1.5	Falling Time Ratio.....	48
8.2	Example Two.....	49
8.2.1	Preliminary Falling Speed	49
8.2.2	Calculation of Lift	50
8.2.3	Calculation of Equilibrium Falling Speed	50
8.2.4	Falling Time Ratio.....	51
9	Conclusions	52
10	Recommendations	54
	Lift of References	55

List of Figures

Figure 3.1:	Force equilibrium with seed in autorotation.....	20
Figure 3.2:	Coefficient of lift as a function of angle of attack for a NACA-2408 airfoil at a Reynolds number of 50000 (Airfoil Tools 2019).....	23
Figure 4.1:	Visual representation of seed element and defined lift generating surface area	24
Figure 4.2:	Contour of a scanned maple seed and division between lift and drag-only generating parts.....	26
Figure 4.3:	Coordinates used to define the upper maple seed contour	26
Figure 4.4:	Plotted equations defining the upper curvature (red), the lower curvature (orange) and the chord length as a function of span (green)	27
Figure 4.5:	Vector diagram defining angle of attack	28
Figure 4.6:	One of the cross-sections used to measure twist compared to a reference plane.....	29
Figure 4.7:	Graph displaying twist as a function of span.....	30
Figure 4.8:	Graph displaying angle of attack as a function of span	31
Figure 4.9:	Post-stall coefficient of lift as a function of angle of attack. The graphs are overlaid with coordinates for use in curve fitting	32
Figure 4.10:	Lift distribution over span obtained for an average maple seed comparing post-stall (green) to conventional (red) $c_L(\alpha)$ use where the purple line represents the end of the maple seed's span	33
Figure 5.1:	Rankine-Froude model of an actuator disk in a free stream (Kulunk 2011)...	35
Figure 7.1:	Falling velocity in air (purple) compared to in free stream (green)	41
Figure 7.2:	Fallen distance in air (purple) compared to in freefall (green).....	42
Figure 7.3:	Fall duration as a function of height in air (purple) compared to in freefall (green)	45

List of Tables

Table 4.1:	Constants used in the chord-span relationship	27
Table 6.1:	Horizontal and vertical normalization constants	37
Table 8.1:	Known parameters of example seed one	45
Table 8.2:	Assumed values for the calculation of preliminary speed one	45
Table 8.3:	Fall durations of example seed one	48
Table 8.4:	Known parameters of example seed two	49
Table 8.5:	Assumed values for the calculation of preliminary speed two	49
Table 8.6:	Fall durations of example seed two	51

List of Symbols

a	Axial induction factor
B	Tip loss correction factor
c	Chord length
\bar{c}	Average chord length
c_{lower}	Lower contour of the maple seed
c_{norm}	Normalized chord length
c_{root}	Chord length at the root of the wing section
c_{upper}	Upper contour of the maple seed
c_D	Coefficient of drag
c_L	Coefficient of lift
D	Drag
F_z	Force of gravity
g	Gravitational constant
h	Height
$k_{norm,hor}$	Horizontal normalization factor of the chord length
$k_{norm,ver}$	Vertical normalization factor of the chord length
$k_{norm,twist}$	Normalization factor of twist
k_{twist}	Constant of twist
L	Lift
m	Mass
\dot{m}	Mass flow rate
p	Pressure
R	Radius as measured from the end of the nut
Re	Reynolds number
R_{tot}	Total span of the wing-section
S_{fluid}	Vertical distance traversed in a fluid
$S_{freefall}$	Vertical distance traversed in freefall
S	Total surface area perpendicular to the vertical flow direction
S_{wing}	Total surface area of the wing section perpendicular to the vertical flow direction
t	Time
Δt_{air}	Fall-time difference in air
$\Delta t_{freefall}$	Fall-time difference in freefall
v_D	Flow velocity at the maple seed
v_{rad}	Circumferential velocity of the point on the rotating object
v_w	Wake flow velocity after maple seed
v_z	Vertical falling velocity in a force equilibrium
$v_{z,preliminary}$	Preliminary value for the vertical falling equilibrium velocity

Greek Symbols

α	Angle of attack
θ_{twist}	Relative angle of twist
$\theta_{norm,twist}$	Normalized relative angle of twist
π	Constant pi
ρ	Density
ν	Kinematic viscosity
ω	Angular velocity

List of Abbreviations

3D	Three-dimensional
BEMT	Blade Element Momentum Theory
CFD	Computational Fluid Dynamics
CoG	Center of Gravity
MATLAB	Matrix Laboratory
NACA	National Advisory Committee for Aeronautics

List of Definitions

Airfoil

A body so shaped as to produce an aerodynamic reaction normal to the direction of its motion through a fluid with minimum drag. (Frénot 1960, pp. 11)

Aspect ratio

The ratio of the square of the span to the gross area of an airfoil. (Frénot 1960, pp. 40)

Asymptote

A straight line that continually approaches a given curve but does not meet it at any finite distance.

Autorotation

A condition of flight wherein there is free and continuous rotation of a helicopter rotor, or other aerodynamic body, caused by air forces and not sustained by engine power inputs. (Frénot 1960, pp. 47)

Camber

Curvature of the median line of an airfoil section; more generally, the curvature of a surface. (Frénot 1960, pp. 79)

Center of mass

A point representing the mean position of the matter in a body or system.

Center of rotation

The center of rotation is a point about which a plane figure rotates.

Chord

The straight line through the centers of curvature of the leading and trailing edges of an airfoil section. (Frénot 1960, pp. 91)

Curve fitting

Curve fitting is the process of constructing a curve, or mathematical function, that has the best fit to a series of data points, possibly subject to constraints.

Drag

The component of the total aerodynamic force in the direction of the undisturbed relative airflow. In powered flight, contributions to this component arising from thrust are excluded. (Frénot 1960, pp. 143).

Lift

The component of the total aerodynamic force in the direction of the lift axis. (**Frénot 1960**, pp. 261)

Span

The distance between the wing tips normal to the plane of symmetry. (**Frénot 1960**, pp. 404)
Here referred to as the total length of the wing section from center of rotation to the wing tip.

Stall

The breakdown of attached flow on a wing or turbomachinery blade leading to marked changes in aerodynamic characteristics, in particular loss of lift. (**Frénot 1960**, pp. 411)

1 Introduction

1.1 Motivation

The study of maple seed aerodynamics has fascinated those in search of improving the current technological efficiencies and engineering fields have often mimicked the mechanics produced by evolution in an attempt to achieve equally high efficiencies.

However, careful design approaches by humans used in conventional design philosophy limit themselves to conventions that originate from the past, resulting in mannerisms that remain unquestioned because “that is how things are done”. This contentment that is found in human design philosophy, letting methods be because they seem to work, need not apply to evolutionary design: an evolutionary design is constantly being put to the test, competing with rivaling mutations that do not limit themselves to changing only the last developed feature of the design. Evolutionary design constantly thinks outside the box because it wouldn’t know where the box even is; being an unconscious process, it requires only an extensive amount of time for such radical trial and error to achieve superb results. We humans do not have the luxury of time that nature does, restricting us to finding an optimal design approach in a time limited context; therefore, we do not constantly question the basis of the design.

Given this discrepancy in design philosophy, designs that are produced by nature often prove to be ingenious in an unconventional way when compared to their more conservative human design equivalents. The efficiencies found in maple seeds in extracting power from the air far exceed their latest man-made equivalents, namely wind turbines; even going so far as to nearly equal the theoretical limit with which power can be extracted from the air. (**Holden 2015**) As a time optimizing species, it would make sense to study the mechanics that are produced by the slow, but still more accomplished process of nature until we have reached an equal design capability. Only then should further research in the mechanics of nature be replaced by starting off where the wisdom of nature has ended, reaching even higher efficiencies on our own or adapting the discovered mechanics to environments where nature has not yet had the time to come up with fitting solutions. As the maple seed still significantly outperforms its man-made equivalents, the most time efficient way of progressing in the field of aerodynamics and design may prove to be the study of such products of nature; perhaps one day allowing us too to extract power from the air at an efficiency close to the theoretical limit.

1.2 Title Terminology

Maple

“A tree or shrub with lobed leaves, winged fruits, and colorful autumn foliage, grown as an ornamental or for its timber or syrupy sap.” (Oxford 2019)

Aerodynamics

“The study of the properties of moving air and the interaction between the air and solid bodies moving through it.” (Oxford 2019)

1.3 Objectives

The main objectives in constructing the methodology are to obtain sufficient accuracy, but moreover a simplicity that allows interpretation of the constructed framework; this would provide the opportunity to extract important insight into the governing mechanics of the autorotation. The goal in sight when solving this research question is not to provide a one-size-fits-all answer which states a global average providing the reduction factor of the fall duration when accounting for air-effects, but rather to both determine the factors which influence this reduction and to mathematically provide relationships that quantitatively display the influence these factors have on it.

A globally averaged answer considering as many maple seeds as possible is thought to be of less value than an answer that allows for the inclusion of individual variances. This is because the subject of maple seed aerodynamics could also appeal to quantitative studies in the field of biology where individual variances are the main driver of survivability; e.g., a study calculating the survivability of the maple tree when shaped by evolution to determine its height and a consequent optimal height. The trade-off between a larger energy need of a taller maple tree and a more effective seed dispersal could show why the tree is as tall as it is found to be. Here, an optimum can only be obtained quantitatively which is where a variance including method would prove to be necessary. Moreover, any study concerning maple seeds will most likely be at an individual level, series of individuals or a normal distribution of geometrical variance; a globally averaged value would thus be of little added value when compared to an individualistic method in such situations.

However, in order to progress from the abstract world of mathematics to real-life applied sciences, exemplar calculations will be made that provide insight into what the physical properties such as lift, falling velocity and the fall duration ratio actually could be in real life examples and to what extent these values vary among seeds with different geometries.

1.4 Literature Review

An overview of existing literature ought to be conducted to find a subject in this narrow topic of research where an added value can be provided. Various publicly available research sources have been consulted using keywords such as “BEMT”, “maple seed” and “post-stall”. The choice of paper was primarily based on the title and it was decided using the abstract whether the paper in question provides an additional perspective on the topic and is therefore suitable for inclusion in this review.

Previous research on this topic fails to provide a simple yet all-encompassing methodology that is able to calculate the aerodynamics of a maple seed from start to finish. However, simulations using CFD and complex mathematical approaches using BEMT have been conducted that describe certain aspects of the seed with reasonable accuracy. **Caley 2013**, **Lee 2017** and **Holden 2015** have simulated maple seeds using CFD with underlying principles of BEMT; whereas **Matič 2015** and **Varshney 2011** have opted for a fundamental approach, each generating a mathematical model that can be used to explain the seed’s mechanics. Although **Matič 2015** and **Varshney 2011** provide some insight into the inner mechanics of the autorotation, the fundamental framework it offers is still fairly limited, discarding the possibility to incorporate important details of the seed into the equations and closing the door to a fundamental discussion of its mechanics.

1.5 Structure

The content of this paper is structured as follows.

- Chapter 2** discusses the recent findings in the field of maple seed research and the possibility of finding an added value
- Chapter 3** derives and provides an equation for the calculation of a preliminary falling speed. This speed will be used later on to give a starting value needed for the calculation of lift. The formula is based on some large assumptions, but it is shown in chapter 3 that the accuracy of this preliminary value is not of large importance.
- Chapter 4** derives and provides the most important equation of the provided methodology, namely the calculation of the lift produced by the falling maple seed. It also discusses and questions the fundamentals of aerodynamical behavior of a maple seed as described by these equations.
- Chapter 5** explains the usage of an equation resulting from BEMT for calculating the actual equilibrium falling speed of a given maple seed.

- Chapter 6** expands the derived equation of lift to a normalized and parametrized version in order to facilitate the use of the provided method.
- Chapter 7** explores a model for calculating the fallen distance of a given maple seed as a function of time based on the calculated falling speed. This fallen distance is then compared to a model describing fallen distance in freefall and subsequent relationships describing the fall duration as a function of height are used to calculate the ratio between the fall duration in air and in freefall.
- Chapter 8** applies the provided equations to two calculation examples of measured maple seeds to give an indication of the accuracy of the derived methodology.
- Chapter 9** summarizes the findings and conclusions that have been derived in the paper and continues with several recommendations for proceeding research

2 State of the Art

Caley 2013 has conducted a research on the CFD simulation using BEMT principles to simulate a maple seed both in rotation and in a steady state with a reasonable level of accuracy. Neither variations in the chord length nor mass have been accounted for in the simulation, undermining accuracy. The paper states that the large variations in the maple seed's geometry lead to extremes in pressure and lift forces, however no framework has been developed to account for these geometrical variations.

Ehrich 2018 compares different methods in their accuracy of solving a multi-megawatt class wind turbine. The three methods are CFD simulation, an actuator line based CFD simulation and a Blade Element Momentum (BEM) approach. It is shown that BEM proves to be the least accurate approach in almost all aspects due to its heavy reliance on significant assumptions.

Holden 2015 analyses the flow field around a maple seed and compares the results to wind turbine blades. It uses empirical values to substitute physical values that were deferred from real life seed samples using high-speed video imaging. Performance values stemming from BEMT show a remarkably high-power coefficient of 0.59 for maple seeds when compared to those ranging from 0.45 to 0.48 commonly found in wind turbines.

Kulunk 2011 discusses fundamental and advanced topics of wind turbine theory. The paper covers subjects ranging from the basic actuator disk model to those including momentum equations (BEMT) and methods of including tip loss correction factors.

Lee 2017 uses the three-dimensional model of a scanned maple seed to numerically simulate the falling velocity and rotational velocity of a maple seed assuming uniform densities for the wing section and for the nut section. The study shows leading-edge vortex (LEV) generation, allowing the seed to attain a high lift force. The study also provides the falling speed and rotational velocity as a function of time. A change in these values for a variance in seed geometry is not accounted for.

Matič 2015 derives a simplified nonlinear dynamic model of a monocopter using a design inspired by a maple seed. The model is based on unsteady BEM theory. A validation is provided by simulation and the results are in good agreement with empirical findings on a qualitative basis, quantitative comparisons validating the constructed method more accurately were not performed. The paper provides a relatively simple approach to explaining many characteristics of the maple seed; however, the progression of falling speed with respect to time is not in agreement with the simulated findings of **Lee 2017**.

Petrilli 2013 provides an aerodynamic database of airfoils and wings at stall and post-stall angles of attack. The paper uses Reynolds-Averaged Navier Stokes (RANS) computational

analysis to simulate high angles of attack lift characteristics providing detailed results for three airfoils. Preliminary calculations and known simulations, conducted by **Lee 2017**, have suggested that a maple seed operates at unconventionally high angles of attack.

Varshney 2011 investigates the kinematics of the transition to a helical motion of a falling maple seed. It discovers that the gyration is not initiated analogously to wind turbines, but that it is rather a three-step process that is only partially dependent on aerodynamical forces. The results produced by **Varshney 2011** limit themselves to be purely qualitative, providing information on the inner mechanics but lacking a quantitative basis.

In reviewing these various sources of research, the conclusion can be stated that the majority of research falls short in providing a theoretical framework that is capable of explaining the fundamental drivers behind the motion that is performed by a maple seed both quantitatively and qualitatively. The inner mechanics of this motion remain largely unexplored and require a solid framework that provides an optimum in combining simplicity and encompassment of maple seed features. Without simplicity, the interpretability will suffer and the possibility of extracting fundamental insights into the mechanics of its workings ought to diminish. However, where the work of **Matič 2015** and **Varshney 2011** fall short is in disregarding a large number of parameters that define the maple seed, therefore oversimplifying not only their model but also the conclusions and insights that can be extracted from it. The geometrical discrepancies among maple seeds have been observed to be of significant influence in defining important parameters such as equilibrium falling speed as has been stated by **Caley 2013**; however, to include these variances has fallen beyond the scope of published papers in this topic research. Previous fundamental research has mainly focused on the application of Blade Element Momentum Theory in search of insights, stemming its understanding from a comparison with wind turbines. However, there are several issues to be formed about BEMT, namely that it is often shown to be an iterative process, that it requires computationally simulated parameters such as the power coefficient and that it relies on a large amount of assumptions as is shown by **Ehrich 2018**. An iterative method, although ought to be avoided, does not necessarily cause great concern, however, in the case of a maple seed any addition of complexity will discourage further inclusion of details that may end up being crucial in providing additional insights. The requirement of computationally simulated parameters strengthens the same argument held against BEMT for use in this case, namely that it provides no insight into the inner mechanics of the flight's workings. Finally, the large amount of assumptions where BEMT is based on may be necessary to alleviate complexity but should be avoided when possible regarding the accuracy of a derived solution. The case held against BEMT seemingly disregards all possibilities of finding a valuable solution for the derivation of a falling speed that attains all requirements, namely accuracy, simplicity, comprehension and flexibility. Therefore, this paper opts to pave the way for an alternative approach in deriving a framework that can be used to solve the required parameters from first principles.

3 Preliminary Equilibrium Falling Velocity

3.1 General Equation

The calculation of a preliminary falling speed requires a simplified model of the forces acting on the maple seed while in a state of falling equilibrium. It can be stated that the force of gravity is the downwards accelerating force which is counteracted by two upwards accelerating forces, namely the force of lift and the force of drag that are produced by the surface as projected in the plane normal to the direction of the fall; as is shown in Figure 3.1.

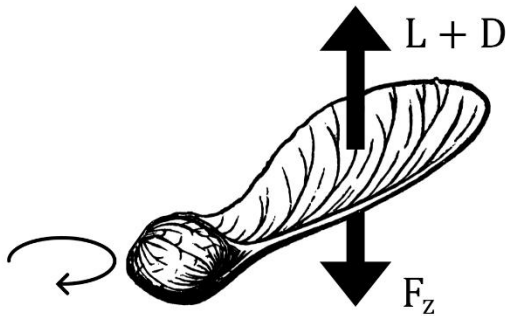


Figure 3.1 Force equilibrium with seed in autorotation

This force balance can be mathematically stated.

$$F_z = L + D \quad (3.1)$$

Which can be expanded from first principles.

$$mg = \frac{1}{2} \rho v_{rad}^2 \cdot c_L \cdot S + \frac{1}{2} \rho v_{z,preliminary}^2 \cdot c_D \cdot S \quad (3.2)$$

Already a simplification has been made concerning the surface area responsible for both lift and drag. In reality the surface area responsible for the generation of drag will be larger than the surface area responsible for lift generation. This is because the inner part of the maple seed consists of a nut containing the actual seed; it can be safely stated that this surface area does not attribute to the generation of lift whereas it does contribute to additional drag generation. However, it is worth emphasizing that this preliminary calculation of an equilibrium falling speed does not need to be highly accurate. There is a tradeoff between accuracy and computational effort and, as will be shown later on, the required accuracy for this preliminary value is not very high so any attempt to increase accuracy and remove simplifications ought to be unnecessary beyond the complexity that this chapter provides.

The radial velocity is dependent on both the angular velocity and the distance to the center of mass, which is also the point of rotation. (**Holden 2015**)

$$v_{rad} = \omega R \quad (3.3)$$

It is worth noting that the used radius, R , must be the distance to the center of rotation. Measurements conducted by **Holden 2015** have shown that the center of rotation and the center of mass lie around the point where the nut ends, and the wing-section of the maple seed commences. Therefore, the radius must be calculated with respect to this general reference point.

If the chord distribution along the axial direction of the maple seed would be of constant length, it would make sense to use half the total radius as an average value for the calculation of the lift force. However, due to an increase in chord length towards the outer edge of the maple seed, the radius of the average airfoil is loosely chosen as 75% of the maximal radius. Therefore, the equation can be derived and consequently simplified.

$$mg = \frac{1}{2}\rho \left(\frac{3}{4}\omega R_{tot}\right)^2 c_L \cdot S + \frac{1}{2}\rho v_{z,preliminary}^2 \cdot c_D \cdot S \quad (3.4)$$

$$mg = \frac{1}{2}\rho S \left[\left(\frac{3}{4}\omega R_{tot}\right)^2 c_L + v_{z,preliminary}^2 c_D \right] \quad (3.5)$$

3.2 Inserting Parameter Values

Depending on the extent to which the user of this method measures and simulates their given maple seed, the possibility exists that this equation can be readily used to calculate a preliminary value for the falling speed. However, in a more likely case only certain parameters such as the mass and total radius will be known values. For the calculation of this preliminary value some empirical substitutions concerning the other variables suffice.

The angular velocity of the maple seed can be assumed to be an averaged value based on empirical data originating from the work of **Holden 2015**, namely 86.29 rad/s.

Given that the height from which the maple seed is released most likely does not exceed the tallest maple tree, it can be safely assumed that conventional values for the gravitational constant and density are appropriate, respectively 9.81 m/s² and 1.225 kg/m³. In extreme conditions regarding temperature, height or pressure it might be relevant to adjust the assumed gravitational constant and density accordingly.

The coefficient of lift is derived from the assumption that a cross-section of the maple seed has the shape of a NACA-2408 airfoil. This type of airfoil was chosen due to its resemblance in thickness and camber to an actual maple seed, although it is worth mentioning that the thickness of a maple seed is far smaller than any known NACA-airfoil. The consequences of having an even thinner than assumed airfoil on the coefficient of lift are thus far unknown.

The coefficient of lift as a function of angle of attack is dependent on the Reynolds number.

$$Re = \frac{v \cdot L}{\nu} \quad (3.6)$$

The Reynolds number can be empirically calculated assuming an ambient air temperature of 15°C. The number will be dependent on the distance to the center of rotation, therefore only the outer extreme will be calculated, as this will provide the largest value. The resulting airspeed will be the vector addition of the horizontal component, caused by rotational velocity, and the vertical component caused by falling speed. To alleviate complexity the Reynolds number is calculated empirically, using values found in the publication of **Varshney 2011**.

$$Re = \frac{\sqrt{(\omega R_{tot})^2 + v_z^2} \cdot L}{\nu} \quad (3.7)$$

$$Re = \frac{\sqrt{(77.9 \frac{\text{rad}}{\text{s}} \cdot 0.029 \text{ m})^2 + (0.94 \frac{\text{m}}{\text{s}})^2} \cdot 2.56 \cdot 10^{-4} \text{ N}}{1.48 \cdot 10^{-5} \frac{\text{m}^2}{\text{s}}} = 2242.27$$

As is to be expected the Reynolds number is very low due to the slow resultant velocity when compared to civil aircraft. The lowest Reynolds number for which data of the coefficient of lift exists, is 50000. It is therefore worth noting that this exceptionally small Reynolds number might undermine the accuracy of this calculation as it is assumed to be over two times higher, namely 50000.

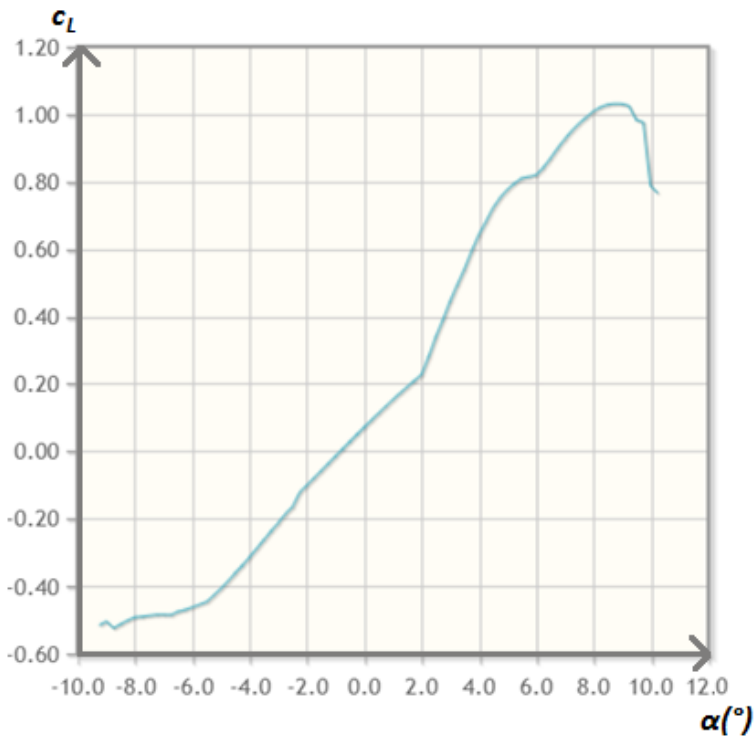


Figure 3.2 Coefficient of lift as a function of angle of attack for a NACA-2408 airfoil at a Reynolds number of 50000 (**Airfoil Tools 2019**)

The largest value of the coefficient of lift occurs around an angle of attack of 8.5° , as is shown in Figure 3.2. As will be discussed later on in Subchapter 3.3, this paper proves that these angles of attack are not relevant for a maple seed; however, for the sake of this preliminary value an arbitrary value that resembles the actual coefficient of lift suffices. Example calculations in Chapter 8 show that assuming a maximal coefficient of lift for this NACA profile results in an accurate preliminary value. The coefficient of lift is therefore assumed to be 1.03 when unknown.

The coefficient of drag can be approximated by regarding the maple seed as a long flat plate perpendicular to the airflow. The resulting value for the coefficient of drag is 1.98 (**Sovran 1978**).

The total surface area can be obtained in several ways, these will be provided in order of decreasing accuracy. Firstly, an effort could be made to precisely measure and calculate the actual surface area of the given maple seed. Otherwise, an approximation could be made using parametrization methods provided by Chapter 6 or an empirical average, derived from the work of **Varshney 2011**, of 579.45 mm^2 can be used.

4 Calculation of Lift

4.1 General Equation

The purpose of Chapter 3 was to provide a preliminary value needed for the calculation of lift, in this chapter the latter will be elaborated. Starting from first principles the basic formula of lift can be stated.

$$L = \frac{1}{2} \rho v^2 \cdot c_L \cdot S \quad (4.1)$$

As explained in Chapter 3, the mentioned velocity refers to circumferential velocity when induced by a rotating object instead of a linear movement. The equation can therefore be adjusted to incorporate this.

$$L = \frac{1}{2} \rho \omega^2 R^2 \cdot c_L \cdot S \quad (4.2)$$

Instead of choosing a value for the average radius as had been previously done, this parameter can be left unknown by using the following method: the total amount of lift generated by the wing area of the maple seed can be viewed as the sum of the infinitesimally small two-dimensional airfoils it consists of. The result is an integral that can be acquired by defining an infinitesimally small surface area, namely $c \cdot dR$.

$$L = \frac{1}{2} \rho \omega^2 \int_0^{R_{tot}} R^2 c_L(R) c(R) dR \quad (4.3)$$

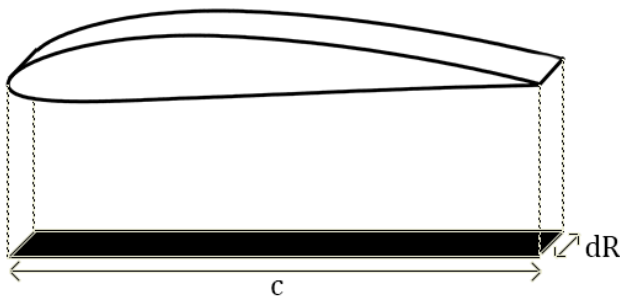


Figure 4.1 Visual representation of seed element and defined lift generating surface area element

Here, the variables that are dependent on the radius at which the two-dimensional airfoil lies, are placed outside of the integral, namely density and angular velocity; whereas the coefficient of lift and the chord length vary along with the radius and are therefore placed inside the integral. The assumption is made that an individual blade element does not influence other blade

elements asides from tip-loss effects and that therefore when the force on every blade element is calculated and summed up, it results in the total force of lift acting on the wing section.

One of the most important three-dimensional effects that can be accounted for is tip loss. A last step in finalizing (3.3) is to account for the tip loss effect that reduces the effective lift due to wingtip vortices. **Wheatley (1934)** suggests a method to account for tip losses.

$$B = 1 - \frac{1}{2} \cdot \frac{\bar{c}}{R_{tot}} \quad (4.4)$$

The method of tip loss correction was chosen from multiple empirical ways of calculating tip losses. Although the equation is empirically devised, it considers parameters that are unlikely of empirical origin in the situation of a maple seed. The equation states that a simplified way of accounting for tip losses is to regard a factor B which states that only B times the wing span is used for effective lift generation. Therefore, (3.3) can be adjusted to include this correction factor.

$$L = \frac{1}{2} \rho \omega^2 \int_0^{B \cdot R_{tot}} R^2 c_L(R) c(R) dR \quad (4.5)$$

From a more realistic point of view, it can be assumed that $c_L(R)$ is not a directly know function. However, a large variety of data providing $c_L(\alpha)$ for many different types of airfoil exists. If the relationship $\alpha(R)$ can be derived, combined with a selection of airfoil as to provide $c_L(\alpha)$, the relationship $c_L(R)$ can be quantitatively obtained.

4.2 Deriving Chord Length

A derivation of the general equation, (3.5), is only part of the work required to transform this method into a practically applicable whole.

A first consideration would be that of the chord length as a function of radius. In order to derive this function, a 3D-model of a laser scanned maple seed was used to create a projection of the wing-surface area as provided by **Hinz 2014**, as can be seen in Figure 4.2.

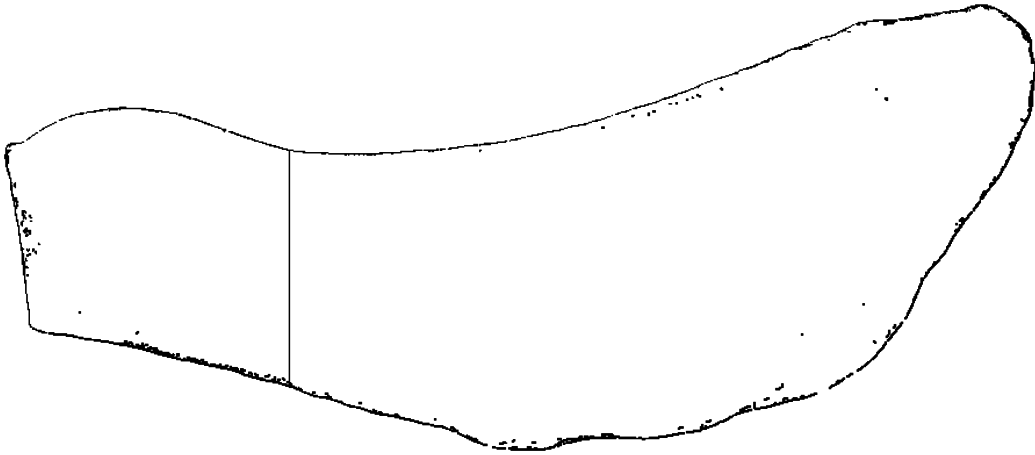


Figure 4.2 Contour of a scanned maple seed and division between lift and drag-only generating parts

The vertical line roughly divides the lift and drag generating part of the seed from its drag-only generating counterpart. An estimation for the positioning of this line was based on measured visual representations of the CoG on actual maple seeds, performed by **Holden 2015**. To transform the contour into an equation viable for use in calculation, coordinates emulating both the upper and lower contour were plotted on the image, shown by Figure 4.3.

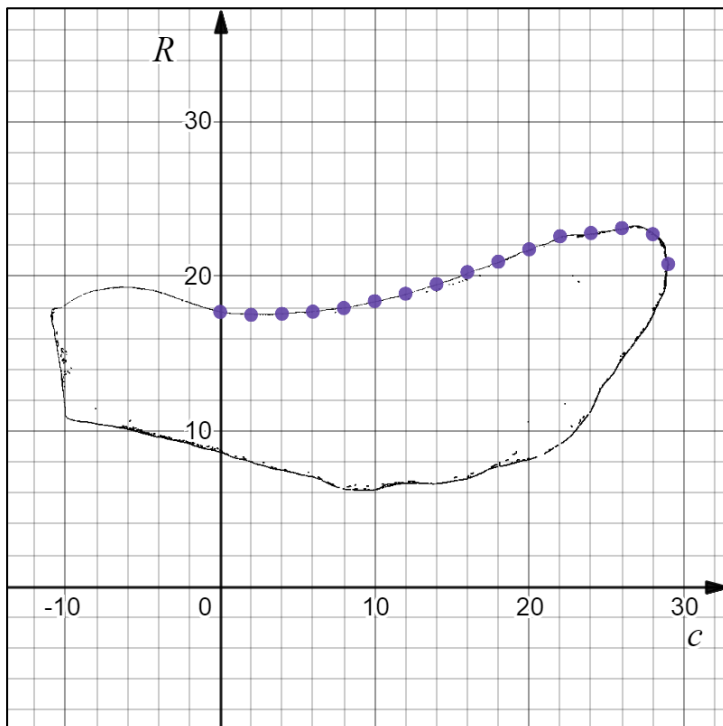


Figure 4.3 Coordinates used to define the upper maple seed contour

The same procedure was followed for approximating the lower contour. Consequently, these two sets of coordinates were inserted in an online curve fitting program, producing two distinct equations. When visually represented by Figure 4.4, these equations approximate the actual contours quite well.

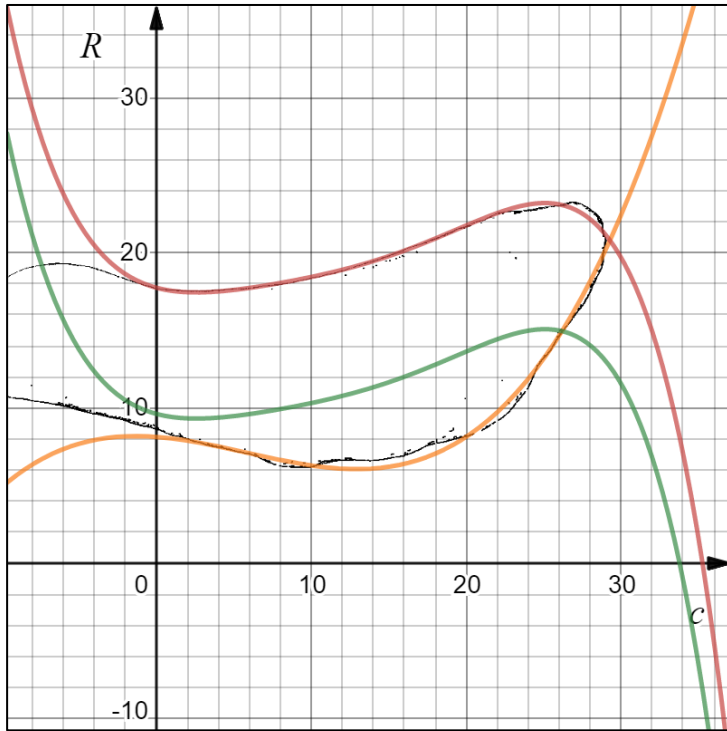


Figure 4.4 Plotted equations defining the upper curvature (red), the lower curvature (orange) and the chord length as a function of span (green)

The green curve represents the subtraction of the equation describing the upper contour from the equation describing the bottom contour, therefore yielding the chord length as a function of span. The represented equations were consequently converted to metric units.

$$c_{upper}(R) = a_1 + b_1R + c_1R^2 + d_1R^3 + e_1R^4 + f_1R^5 \quad (4.6)$$

$$c_{lower}(R) = a_2 + b_2R + c_2R^2 + d_2R^3 \quad (4.7)$$

$$c(R) = c_{upper}(R) - c_{lower}(R) \quad (4.8)$$

$$\Leftrightarrow c(R) = a_3 + b_3R + c_3R^2 + d_3R^3 + e_3R^4 + f_3R^5 \quad (4.9)$$

Table 4.1 Constants used in the chord-span relationship

	a	b	c	d	e	f
1	0.01774875	-0.267276	72.85199	-6395.706	299436.6	5163319
2	0.008131709	-0.07557199	-25.45918	1462.664		
3	0.009617041	-0.34284799	47.39281	-4933.042	299436.6	5163319

When information of the geometry of the maple seed is unknown, the given $c(R)$ relation, using Table 4.1, can be used to approximate the chord as a function of span. However, a more accurate method would be to adjust this function to match certain parameters of the seed's geometry. An adaptation of this function can therefore be found in Chapter 6.

4.3 Deriving Angle of Attack

As previously discussed, the retrieval of the relationship $c_L(R)$ will require a derivation of $\alpha(R)$ first. The angle of attack is defined as the relative angle at which the air interacts with the airfoil. This can be solved by finding the angle between the velocity vector responsible for downwards motion and the perpendicular velocity vector responsible for angular motion.

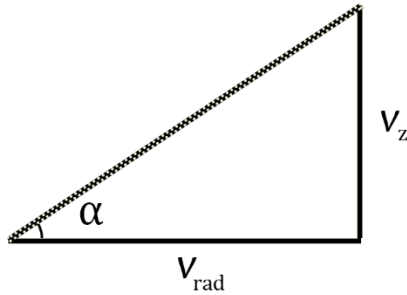


Figure 4.5 Vector diagram defining angle of attack

$$\tan(\alpha) = \frac{v_z}{v_{rad}} \quad (4.10)$$

As previously discussed in a body acting out a rotational movement, the circumferential velocity is defined as the product of angular velocity and the radius.

$$\tan(\alpha) = \frac{v_z}{\omega R} \quad (4.11)$$

Or when transformed to describe the angle of attack, the equation alters to

$$\alpha = \tan^{-1}\left(\frac{v_z}{\omega R}\right) . \quad (4.12)$$

A final step towards improving compatibility with the coming $c_L(\alpha)$ equation requires us to change the unit to degrees instead of radials. This can be accomplished through multiplication with a prescribed factor of $\frac{180}{\pi}$.

$$\alpha = \tan^{-1}\left(\frac{v_z}{\omega R}\right) \cdot \frac{180}{\pi} \quad (4.13)$$

The dependency of the angle of attack on the falling speed gives rise to a problem. Namely, if the method of calculation of a falling speed requires the falling speed itself as an input parameter, then it can only be solved by means of a preliminary value, iterations and a hope of convergence. It is for this reason that the preliminary value discussed in Chapter 3 is calculated. However, it turns out that variances of this inserted falling speed affect the outputted value of

lift only to a very small extent, as is shown in Chapter 8. A further iteration after the first calculation of the definitive falling speed therefore turns out to be unnecessary.

A geometrical twist can be included when it is considered as a relative deviation in angle of attack as a function of span. A measurement of a regular twist has been made on the same three-dimensional model of a scanned maple seed, provided by **Hinz 2014**. For this purpose, 36 cross-sections were made of the maple seed and laid over a fixed frame of reference, shown by Figure 4.6.

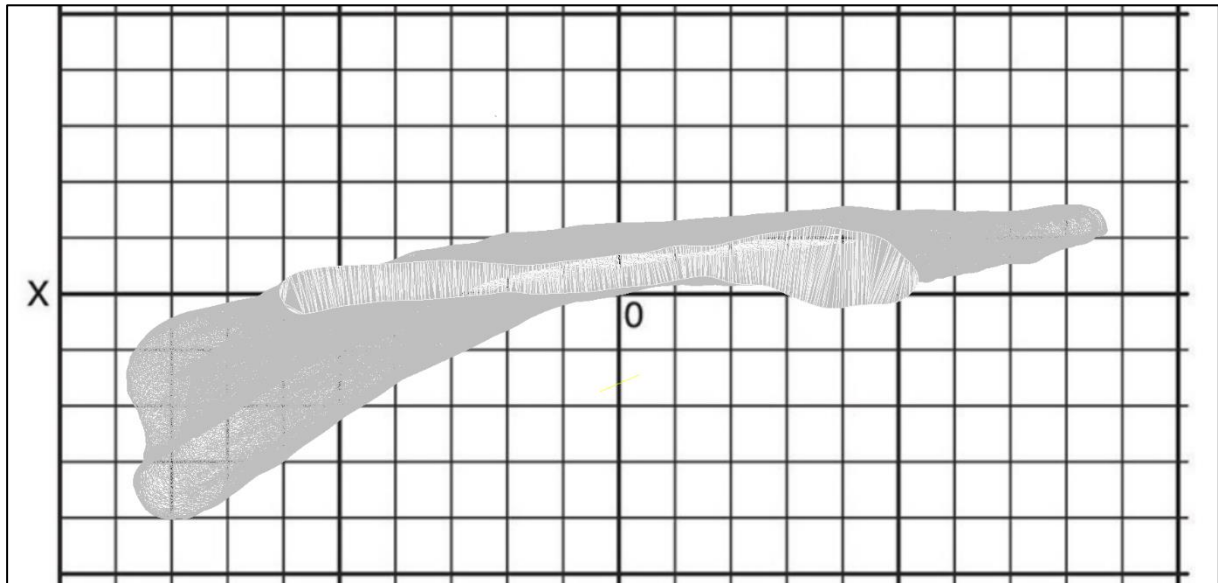


Figure 4.6 One of the cross-sections used to measure twist angle overlaid on a reference plane

Using Adobe Photoshop CS6, the angle between the chord and horizontal reference line was carefully measured for every frame resulting in a set of coordinates representing the relative angle to the horizontals of this frame of reference. Afterwards, these values were inserted into an online curve fitting tool to obtain the twist over span relationship mathematically.

$$\theta_{twist}(R) = -2.643338 + 2222.355 \cdot R - 78527.12 \cdot R^2 \quad (4.14)$$

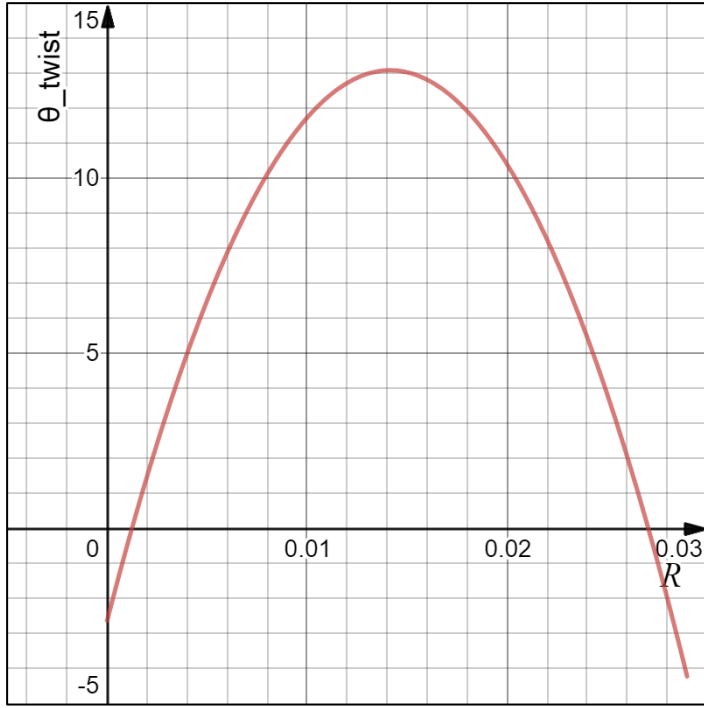


Figure 4.7 Graph displaying twist as a function of span

As can be seen, it is assumed that the twist commences at an angle of -2.643° . This is due to the arbitrary frame of reference that is chosen. In reality, it is unknown to the extent of this paper at which angle the root of the wing-section travels while in stable autorotation. To be precise, this uncertainty introduces an unknown variable which is denoted as k_{twist} , so that when this variable equals 2.643, the root is traveling at an angle that doesn't deviate from the plane of rotation. The complete equation describing the angle of attack therefore becomes

$$\alpha(R) = \tan^{-1}\left(\frac{v_z}{\omega R}\right) \cdot \frac{180}{\pi} + \theta_{twist}(R) + k_{twist} \quad (4.15)$$

It is assumed in this paper that the constant of twist, k_{twist} , is equal to zero.

When objectively analyzed this curvature of twist is not the way conventional geometrical twist develops along the span: it is expected to go from a high angle of twist to a low angle of twist to compensate the higher circumferential velocities towards the tip. In the case of the maple seed, the twist is shown to oddly increase before it decreases. An explanation for this phenomenon lies outside the scope of this paper and is a topic for further research.

For the sake of understanding the mechanisms that drive the autorotation of a maple seed, the angle of attack as a function of span can be plotted for an average maple seed, shown by Figure 4.8. Here, the angular velocity is chosen as 77.9 rad/s with a falling speed equal to 0.94 m/s as is shown to be regular values found in the work of **Varshney 2011**.

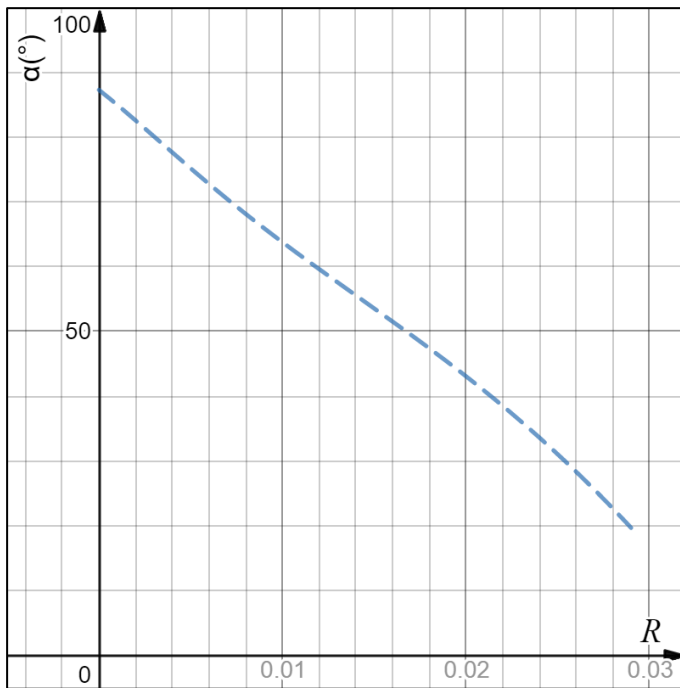


Figure 4.8 Graph displaying angle of attack as a function of span

Traditional knowledge of autorotation implies that conventionally only a small portion of the helicopter blade can be generating lift. This phenomenon occurs because the angle of attack is significantly dependent on the radius, where towards the span it is found that the angle of attack decreases due to a greater circumferential velocity. This variance in angle of attack is so large that when applied to the traditional function for obtaining the coefficient of lift in relation to angle of attack, most of the conventional wing (55%) falls outside of usable angles of attack. A normal range of usable angles of attack, yielding positive coefficients of lift, would be from a slightly negative, say -3° , to around 12° . However, when the angles of attack for the maple seed are observed, they range from 90° to 19.64° for a twist constant of zero. The obvious explanation would be to assume that the chosen constant of twist is therefore wrong and needs to be a large negative value, however, this turns out to defy evidence shown by experiments and simulations made of maple seeds in autorotation. Carefully observed simulations of Lee 2017 show that the root of the wing-section crosses the air mass at a somewhat horizontal angle, not a large negative angle.

The mystery of the angle of attack is solved when stepping out of the traditional frame of thinking; post stall angles of attack are generally neglected in aircraft and helicopter design due to an emphasis on the excessive production of drag; however, this manner of thinking does not need to apply to a maple seed. The drag produced may very well be necessary to enter a stable angular velocity, but the biggest advantage lies in a much more efficient use of lift, as will be explained in Chapter 4.4.

4.4 Deriving the Coefficient of Lift

To implement this post stall approach, the relationship $c_L(\alpha)$ needed to be obtained for a certain airfoil resembling the maple seed's cross section. The even smaller amount of public data on post-stall characteristics on airfoils is a severe limitation to this research, although a chart had been found originating from the work of **Petrilli 2013** providing the relationship for three distinct airfoils, namely NACA 4415, NACA 0012 and NACA 63006. Out of these three airfoils, the NACA 4415 was selected because of its positive camber. This feature of positive camber is distinctly visible when observing a maple seed. Again, the limitation is worth noting that a NACA 4415 airfoil is significantly thicker than a maple seed.

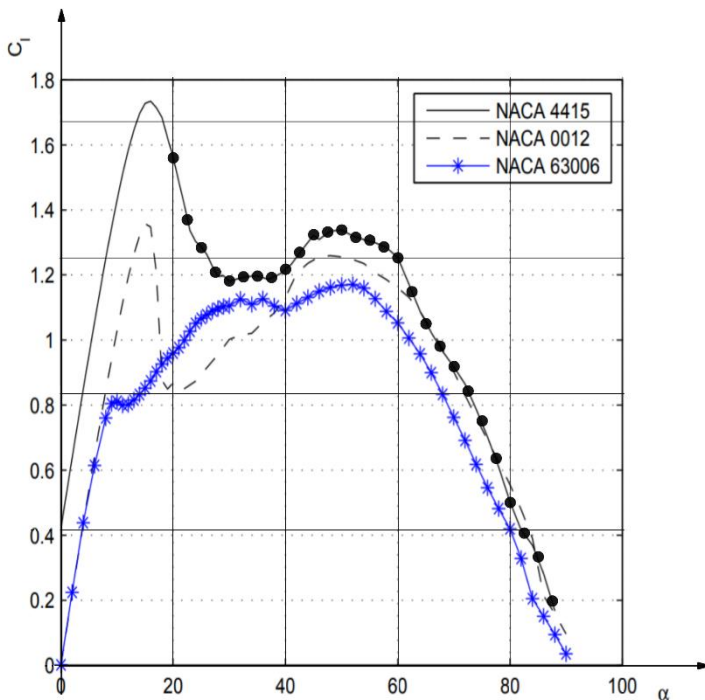


Figure 4.9 Post-stall coefficient of lift as a function of angle of attack. The graphs are overlaid with coordinates for use in curve fitting

Figure 4.9 displays the NACA 4415 $c_L(\alpha)$ relationship, overlaid by the coordinates that were used to curve fit the graph. In order to improve accuracy of the curve fit, only the range of angles of attack which is used in the maple seed was inserted into the curve fitting tool.

$$c_L(\alpha) = 5.450 - 0.373 \cdot \alpha + 0.0114 \cdot \alpha^2 - 0.000142 \cdot \alpha^3 + 6.096 \cdot 10^{-7} \cdot \alpha^4 \quad (4.16)$$

With this equation given, an effort can be made to display the progression of the coefficient of lift along the span of an average maple seed. Again, the chosen angular velocity and falling speed are respectively 77.9 rad/s and 0.94 m/s.

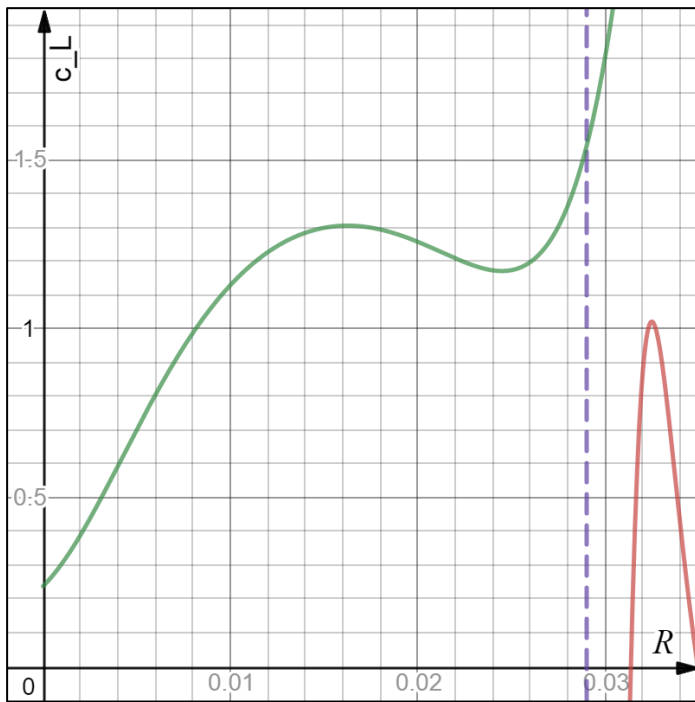


Figure 4.10 Lift distribution over span obtained for an average maple seed comparing post-stall (green) to conventional (red) $c_L(\alpha)$ use where the purple line represents the end of the maple seed's span

A comparison is made with the application of the same method but for a curve fit to a normal range of angles of attack, namely between -3° and 12° , shown by Figure 4.10. The result is that when fitted to the conventional range only a very narrow section of the wing will be developing lift, a far too narrow region to slow the seed down effectively. Moreover, this conventional range of angles of attack falls beyond the span of the maple seed, stating that the maple seed produces no lift whatsoever. In contrary, when fitted to a post stall curvature of $c_L(\alpha)$, the maple seed will produce a very broad and positive area of lift as is shown by the green curve. The supporting evidence for this theory comes from the fact that the constant of twist can be held zero, confirming visual evidence of falling seeds shown by **Lee 2017**, while still producing a large enough amount of lift. Another seemingly implausible fact that follows is that not a single cross-section of the seed will be positioned in an optimal angle of attack of around 12° ; however, there is no need for this because the wider range of positive c_L that can be achieved using post stall angles of attack proves to be a larger advantage than having a higher maximal value.

The other values required to compute the lift are density, angular velocity and total radius. The density can be presumed 1.225 kg/m^3 given that the same logic applies that was previously discussed in Chapter 3. The angular velocity, unless measured, is a significant limitation of this method of calculation. The current approach is to use an empirical average value of 86.29 rad/s unless the value is known to be otherwise, as is shown to be an empirical average using values from the paper written by **Holden 2015**. The discovery of a relationship between angular velocity and other known parameters would aid this method in becoming more fundamentally based, unfortunately this remains yet to be accomplished in further research. The method was devised with the idea that the total radius (as measured from the end of the nut) can be measured

and is therefore left as one of the key unknown variables influencing the falling speed, however when used otherwise than intended it can be assumed to be 0.029 m as is shown to be an average value stemming from results generated by **Holden 2015**.

5 Using BEMT to Calculate Falling Velocity

The basis of Blade Element Momentum Theory is given by the Rankine-Froude model of a wind turbine.

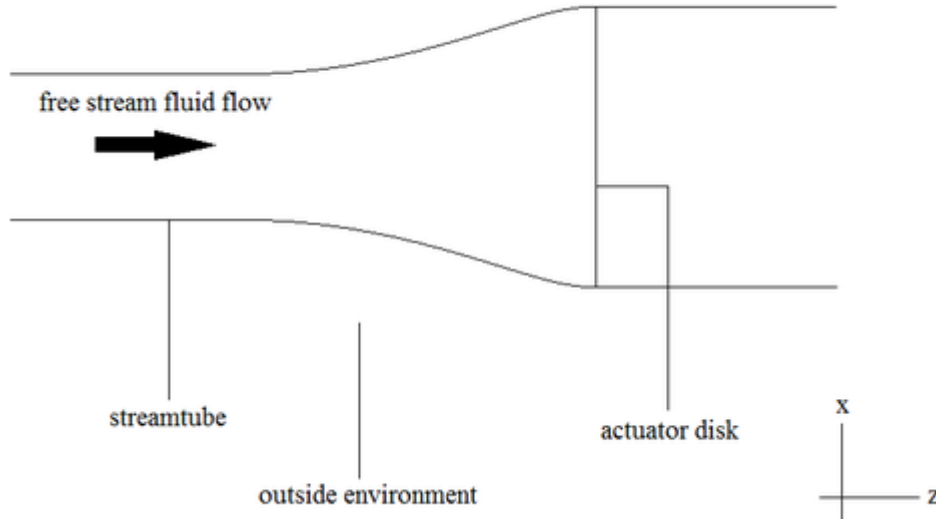


Figure 5.1 Rankine-Froude model of an actuator disk in a free stream (Kulunk 2011)

The simplified interpretation of Figure 5.1 can be used to consider a maple seed surface as if it were such an actuator disk. Here, a free stream fluid flow interacts with the actuator disk transferring its energy onto the rotor. Consequently, the rotor uses this energy to initiate an angular motion and to generate a thrust, or in our case lift.

The major consideration is that unlike the wind turbine, the maple seed itself induces this relative fluid velocity by falling; however, for aerodynamical purposes this is of little relevance.

The rotor extracts a force from the fluid which is denoted as lift instead of the common denotation of thrust as is found in wind turbine theory.

$$L = \frac{dp}{dt} \quad (5.1)$$

Where dp/dt refers to the rate of change in axial momentum, resulting in a lift force. A more convenient notation of this rate of change would be to use the product of mass flow of the free stream and the velocity difference before and after the actuator disk. (Kulunk 2011)

$$L = \dot{m} \cdot (v_z - v_w) \quad (5.2)$$

Classical physics states that the mass flow rate can be expressed as a function of the area, density and velocity of the point of the actuator disk or in this case at the point of the maple seed.

$$L = \rho S v_D \cdot (v_z - v_w) \quad (5.3)$$

Furthermore, the wake velocity can be expressed in terms of the axial induction factor, a , and the free flow velocity. (**Kulunk 2011**)

$$v_w = (1 - 2a) \cdot v_z \quad (5.4)$$

Combining the previous two equations provides an equation that is suitable for calculating the actual falling speed of the maple seed.

$L = \rho S v_z^2 \cdot (2a - 2a^2) \quad (5.5)$
--

The only thus far unknown parameter required to calculate the falling speed is the axial induction factor, a , which accounts for the deceleration of the fluid when approaching the maple seed surface. The axial induction factor of a maple seed has been calculated by **Holden 2015** using CFD and was shown to be 0.313. Not including a change in axial induction factor when a change of geometrical variables occurs, is something that might significantly undermine the added value of this paper, namely its encompassment of geometrical variables. Every effort ought to be made to investigate the influence these geometrical variances have on important parameters; however, for the sake of this paper it is unrealistic to provide an inclusion of geometry in the shaping of the axial induction factor since it is numerically simulated in the case of a maple seed. The assumption is therefore made that the axial induction factor remains the same for every available maple seed since it relates to the power coefficient. The power coefficient is synonymous to efficiency; therefore, it can be assumed that the power coefficient and thus the axial induction factor are evolutionarily designed to be constant for every maple seed in such a way that the efficiency with which the seed extracts power from the air remains the optimal value of 0.313, evolutionarily altering its geometry to achieve this goal.

6 Parametrization of Lift Formula

In order to provide a more practical variant of this method, the general equation calculating lift has been adapted to have simplified geometrical parameters as input variables to facilitate the use of this method. For example, a limitation is that the chord-span relationship, namely $c(R)$, requires the user to either define a function approximating this relationship themselves by careful measurement of the given maple seed or to plainly use the provided relationship of the maple seed that has been used for the approximation of this paper. Looking at this problem from an abstract perspective it can be said that the user can either go through a lot of effort to achieve a large amount of accuracy or the user can use the ready-made function, being satisfied with a low amount of accuracy. However, as of now there is no in-between method, using some deviation from the actual geometry but with an easier implementation of the method. In order to fill this lacuna, this parametrization method was developed.

The two most important parameters defining the shape of the maple seed are the total wingspan as measured from the end of the nut, denoted by R_{tot} , and the chord length of the maple seed at its root, denoted by c_{root} . Using solely these two parameters, a large number of geometrical variables can be adjusted to be in better accordance with the given maple seed.

6.1 Parametrizing Chord Length

Firstly, the function $c(R)$ ought to be normalized to provide an easy to use parametrized equation. To normalize the function horizontally it can be stated that

$$c(1 \cdot k_{norm,hor}) = 0 \quad . \quad (6.1)$$

A correction factor is defined that horizontally scales the chord function so that the chord length is zero when the radius is equal to one. Another correction factor can be defined that vertically scales the chord function so that at a radius of zero, the chord length is equal to one. The values of these correction factors are given by Table 6.1.

$$k_{norm,ver} \cdot c(0) = 1 \quad (6.2)$$

Table 6.1 Horizontal and vertical normalization constants

$k_{norm,hor}$	$k_{norm,ver}$
0.029278	103.983

When implemented into the equation describing chord length as a function of radius, a normalized version can be obtained.

$$c_{norm}(R) = -11.550 \cdot R^5 + 22.878 \cdot R^4 - 20.507 \cdot R^3 + 8.7628 \cdot R^2 - 0.58365 \cdot R + 1 \quad (6.3)$$

The normalized function can be easily adjusted to the maple seed shape given by the defined geometrical parameters, using

$$c_{root} \cdot c_{norm}\left(\frac{R}{R_{tot}}\right) \quad (6.4)$$

6.2 Parametrizing Twist

The equation describing twist as a function of span, namely (4.14), has been constructed so that it fits to a maple seed with a total radius equal to 29 mm. However, since R_{tot} has been defined as an input parameter, this equation too can be adjusted so that to R_{tot} can be left unknown. Firstly, the twist equation will be normalized to facilitate the implementation of this parameter.

$$\theta_{twist}(k_{norm,twist} \cdot 1) = 0 \quad (6.5)$$

The horizontal scaling factor states from the given equation that when normalized, the twist equals zero when the radius is equal to one meter. When computed, correction factor $k_{norm,twist}$ is required to have a value of 0.027056.

$$\theta_{norm,twist}(R) = \theta_{twist}(k_{norm,twist} \cdot R) \quad (6.6)$$

$$\theta_{norm,twist}(R) = -2.643338 + 60.128 \cdot R - 57.484 \cdot R^2 \quad (6.7)$$

Because of this normalization, an easy to use relationship accounting for this unknown R_{tot} can be created.

$$\theta_{norm,twist}\left(\frac{R}{R_{tot}}\right) \quad (6.8)$$

The adjusted function is to be used when parameter R_{tot} is known instead of the fixed equation describing twist as a function of span, (4.14).

6.3 Parametrizing Total Surface Area and Tip Loss Correction

Using the adjusted equation describing chord length as a function of span, a new value of wing surface area can be calculated by integrating the chord length along the total span. This value can be used both in the preliminary falling speed, although this may not be necessary, but more importantly when calculating the definitive falling speed.

$$S_{wing} = \int_0^{R_{tot}} c_{root} \cdot c_{norm} \left(\frac{R}{R_{tot}} \right) dR \quad (6.9)$$

When calculating the total surface area required for the final falling velocity, an empirical value for the nut surface area can be used and added to the calculated wing surface area. It is shown that when the nut is cut away from an average maple seed, the surface area is reduced by 59.2 mm² (Varshney 2011). The total wing surface area can therefore be approximated using

$$S = 5.92 \cdot 10^{-5} + \int_0^{R_{tot}} c_{root} \cdot c_{norm} \left(\frac{R}{R_{tot}} \right) dR \quad (6.10)$$

A final and minor adjustment can be made using this method of parametrization, concerning the tip loss correction factor B . This correction factor uses the mean chord length and total wing span, which can be formulated in accordance with the defined parameters.

$$\bar{c} = \frac{\int_0^{R_{tot}} c_{root} \cdot c_{norm} \left(\frac{R}{R_{tot}} \right) dR}{R_{tot}} \quad (6.11)$$

Using the adjusted function describing chord length, a more accurate average value for the chord length can be obtained. The effective amount of surface area that is used will be approximated more accurately when accounted for this new value. Hereafter, (4.4) is to be applied using the new value for the averaged chord length, namely

$$B = 1 - \frac{1}{2} \cdot \frac{\bar{c}}{R_{tot}} \quad .$$

7 Calculation of Fallen Distance

7.1 Fallen Distance Including Aerodynamic Effects

In order to complete the task of providing an all-encompassing framework to describe the aerodynamics and mechanics of a maple seed, the sole calculation of the equilibrium falling speed does not suffice. Preceding this state of force equilibrium, the seed will be in a transient state where the forces of drag and lift gradually build up until they cancel out the acceleration caused by the force of gravity. A lack of data to empirically approximate the forces during this transient period dismisses the possibility to solve this problem in an empirical fashion, whereas a fundamentally based solution falls beyond the scope of this paper and could be considered a task for further research.

In fact, only a relatively small amount of information is known about the relationship of falling speed as a function of time for maple seeds. Namely that it gradually reaches a falling speed equal to the calculated equilibrium speed after a timespan that is not overly long, that the acceleration when dropped is equal to the earth's acceleration and that the initial vertical velocity is equal to zero.

Mathematically, this set of constraints can be constructed as

$$\lim_{t \rightarrow +\infty} v(t) = v_z \wedge \frac{d v(t_0)}{dt} = g \wedge v(0) = 0 \quad . \quad (7.1)$$

One function suitable for approximation of such a relationship is a scaled hyperbola.

$$v(t) = \frac{1}{-(k_a t + k_b)} + k_c \quad (7.2)$$

Here, three constants are defined that can be solved using the three defined constraints. Firstly, when calculated, the velocity value of the horizontal asymptote is found to be equal to the constant k_c . It can therefore be stated that this constant k_c is equal to the equilibrium falling speed, v_z .

The second constraint can be used to define a relationship between k_a , k_b and the gravitational constant g .

$$\frac{dv(t)}{dt} = \frac{d \left[\frac{1}{-(k_a t + k_b)} + v_z \right]}{dt} = \frac{k_a}{(k_a t + k_b)^2} \quad (7.3)$$

This derivative is ought to be equal to the gravitational constant, g , when t is equal to zero.

$$g = \frac{k_a}{(k_a \cdot 0 + k_b)^2} \Leftrightarrow g = \frac{k_a}{k_b^2} \quad (7.4)$$

The third constraint, defining the origin point, can be used to obtain the value for constant k_b .

$$v(0) = 0 \quad (7.5)$$

$$\Leftrightarrow \frac{1}{-(k_a \cdot 0 + k_b)} + v_z = 0 \Leftrightarrow k_b = \frac{1}{v_z} \quad (7.6)$$

Using the relationship of g to k_a and k_b , the value of k_b can be used to obtain the value of k_a .

$$g = v_z^2 k_a \Leftrightarrow k_a = \frac{g}{v_z^2} \quad (7.7)$$

Therefore, the equation describing $v(t)$ can be written and simplified as

$$v(t) = v_z - \frac{v_z^2}{gt + v_z} \quad (7.8)$$

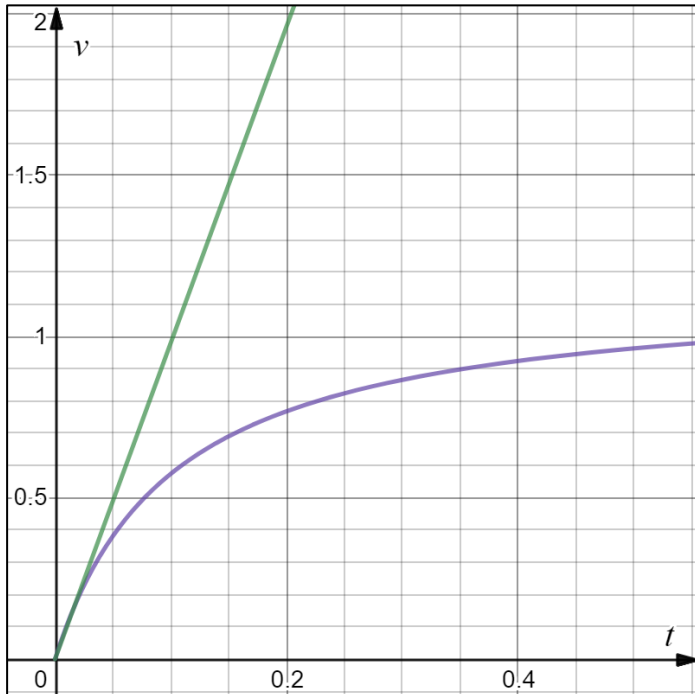


Figure 7.1 Falling velocity in air (purple) compared to in free stream (green)

From this relationship describing falling speed as a function of time, the vertical distance that the maple seed has traversed in its falling motion can be derived by taking the integral of the calculated function.

$$s_{fluid}(t) = \int v(t)dt \quad (7.9)$$

$$s_{fluid}(t) = v_z t - \frac{v_z^2 \cdot \ln(gt + v_z)}{g} + C \quad (7.10)$$

For practical purposes the requirement to take the absolute value inside of the natural logarithm has been disregarded, since the value of $gt + v_z$ always is a positive value. The integration introduces an integration constant that needs to be solved, defining the vertical displacement of the function. A constraint, defining constant C is that the function should pass the origin, mathematically this constraint can be stated as

$$s_{fluid}(0) = 0 . \quad (7.11)$$

Therefore, the resulting equation becomes

$$s_{fluid}(t) = v_z t - \frac{v_z^2 \cdot \ln(gt + v_z)}{g} + \frac{v_z^2 \cdot \ln(v_z)}{g} . \quad (7.12)$$

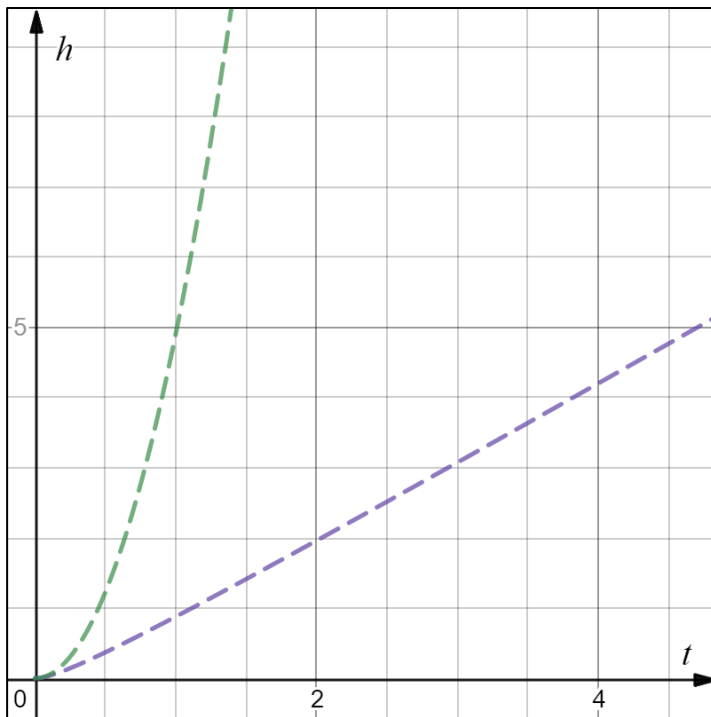


Figure 7.2 Fallen distance in air (purple) compared to in freefall (green)

7.2 Fallen Distance in Freefall

In order to compare a maple seed under the effect of aerodynamic influences to a maple seed in freefall, a simple framework providing the fallen distance in freefall has been developed.

While in freefall, the only force acting on the maple seed is the force of gravity, denoted as F_z . The aerodynamic forces of drag and lift that were previously used for stating the vertical falling equilibrium are therefore dismissed. If only one downwards pulling force is exerted on the seed, then a state of force equilibrium is never reached which results in a constant acceleration, equal the gravitational constant g . Evaluating the double integral of this acceleration as a function of time will provide the relationship describing traversed vertical distance as a function of time.

$$s_{freefall}(t) = \iint g dt = \frac{gt^2}{2} \quad (7.11)$$

7.3 Falling Time Ratio

In order to answer the research question, “How much longer the seed falls using autorotational principles when compared to freefall?”, a general equation can be formulated that provides a ratio comparing the time it takes for a given maple seed to fall from a certain height in air to the time it takes for that same maple seed to fall from the same height in freefall.

Firstly, both (7.10) and (7.11) ought to be inversed to provide the traversed vertical distance, or height, as a function of time. During freefall, the fall duration as a function of height is expressed as

$$\Delta t_{freefall} = \sqrt{\frac{2 \cdot h}{g}} \quad (7.12)$$

Unfortunately, the function describing this relationship in air can not be as cleanly inversed and turns out to be a relationship providing two values for the fall duration for a given height, of which one is negative and thus clearly false.

$$\ln(g \cdot \Delta t_{air} + v_z) v_z^2 - g v_z \cdot \Delta t_{air} - v_z^2 \ln(v_z) + gh = 0 \quad (7.13)$$

The inconvenience of a relationship that provides a false and a true value can be resolved by taking the absolute value of the term that allows for this negative duration.

$$|\ln(g \cdot \Delta t_{air} + v_z) v_z^2| - g v_z \cdot \Delta t_{air} - v_z^2 \ln(v_z) + gh = 0 \quad (7.14)$$

The trade-off is that the duration will be a slightly wrong value when the equilibrium falling speed is below 1 m/s. The obtained value for Δt_{air} will be false until

$$\Delta t_{air} = \frac{v_z(v_z \cdot \ln(v_z) - v_z + 1)}{g} . \quad (7.15)$$

When this value of Δt_{air} is calculated for calculation example one, with values stemming from Subchapter 8.1, it is found to be equal to 176 μs . Conclusively, this interval of error is therefore negligible when calculating practical examples.

Using the same conventional values for v_z and g , namely 0.94 m/s and 9.81 m/s², these relationships can be visually compared.

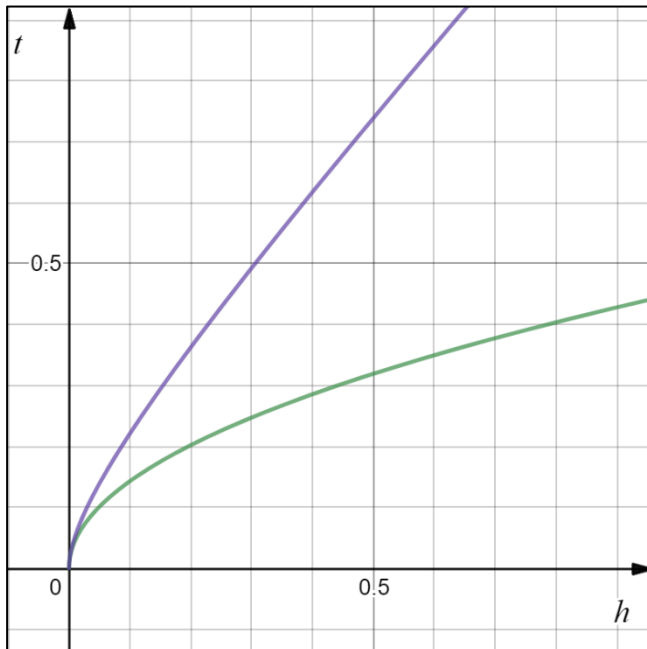


Figure 7.3 Fall duration as a function of height in air (purple) compared to in freefall (green)

Unfortunately, because the fall duration in air cannot be cleanly expressed as a function, it cannot be used to construct an equation that calculates the ratio prescribing how much longer a seed falls in air when compared to in freefall; however, this does not imply that such a ratio cannot be calculated, as will be demonstrated in Sections 8.1.5 and 8.2.4.

As can be observed in the above graph, the time difference between both fall durations increases more for a given increase of height than the fall duration in freefall does. This implies that the falling time ratio increases with an increase in height since the seed will have had percentage-wise more time in a state of autorotation.

8 Calculation Examples

8.1 Example One

Based on a research concerning the kinematics of falling maple seeds, namely that of **Varshney 2011**, a sufficient number of parameters has been obtained of two distinct maple seeds. The researchers released these maple seeds and precisely measured their falling speeds. Because both seeds have very different falling speeds given due to their distinct geometries, they prove excellent examples to verify the constructed method. It is worth noting that not all parameters that are open for use in the method were provided by the research paper. A very high amount of accuracy is therefore not expected, but a relative approximation and a clear sign of the influence of the difference in geometry will suffice.

The information available for the first maple seed is a select, but important number of parameters, given by Table 8.1.

Table 8.1 Known parameters of example seed one

m (mg)	S (mm ²)	ω (rad/s)	v_z (m/s)
170.6	612.8	77.9	0.94

Unfortunately, due to the small number of known variables, the parametrization equations cannot be used to achieve a higher amount of accuracy.

8.1.1 Preliminary Falling Speed

Firstly, the equation for the calculation of this preliminary falling speed can be restated, namely (3.5).

$$mg = \frac{1}{2} \rho S \cdot \left[\left(\frac{3}{4} \omega R_{tot} \right)^2 \cdot c_L + v_{z,preliminary}^2 c_D \right]$$

The only unknown geometrically based parameter is the total radius, R_{tot} , which can be empirically approximated to be 29 mm, as is discussed in Subchapter 3.2. Besides from that, the other unknown values are expected to be unknown and will be assumed to be the values that have been prescribed in Subchapter 3.2.

Table 8.2 Assumed values for the calculation of preliminary speed one

g (m/s ²)	ρ (kg/m ³)	c_L	c_D
9.81	1.225	1.0586	1.98

Using these input values, the general equation can be solved to provide a preliminary value for the falling speed, namely $v_{z,preliminary}$.

$$\Leftrightarrow v_{z,preliminary} = 0.842 \frac{\text{m}}{\text{s}}$$

8.1.2 Calculation of Lift

Using this preliminary value of falling velocity during force equilibrium, the general equation of lift can be restated as follows and consequently solved using (4.5).

$$L = \frac{1}{2} \rho \omega^2 \int_0^{B \cdot R_{tot}} R^2 c_L(R) c(R) dR$$

Firstly, the tip loss correction factor should be calculated using the same logic as is explained in Subchapter 6.3.

$$\bar{c} = \frac{\int_0^{R_{tot}} c(R) dr}{R_{tot}}$$

The average chord will be calculated using the empirical values given by the maple seed of which the relationship $c(R)$ was measured as previously discussed in Chapter 4. A keen observer might state that the value given by the integral can be corrected so that it is consistent with the known total surface area. However, since this tip loss correction factor is dependent on the aspect ratio, adjusting only the average chord and not the total wingspan to fit the given maple seed will in fact cause the correction factor to be even less accurate than if it was calculated on a purely empirical basis. Therefore, the provided equation describing a standard chord length progression along the span is used, combined with an average total wingspan of 0.029 m as is recommended in Subchapter 4.4.

$$\bar{c} = \frac{\int_0^{0.029} c(R) dr}{0.029} = 0.01189 \text{ m}$$

The tip loss correction factor B , using (4.4), can therefore be computed.

$$B = 1 - \frac{\bar{c}}{2R_{tot}} = 0.807086$$

According to this empirical value, only 80.7% of the wing span of an average maple seed is effectively used for generating lift.

Aside from this, there is no need to further calculate any variables; therefore, MATLAB was used to compute the value of lift. The empirical relation describing twist as a function of radius remained unadjusted due to the total radius being left unknown. Using (4.14), the function describing angle of attack as a function of radius can be stated, where the preliminary velocity is substituted as 0.842 m/s as is calculated. This equation can then be inserted into the function describing $c_L(\alpha)$ and combined with the empirical equation describing chord as a function of radius, (4.9), a value of lift can be computed.

$$L = \frac{1}{2} \rho \omega^2 \int_0^{B \cdot R_{tot}} R^2 c_L(R) c(R) dR$$

$$L = 2.5493 \cdot 10^{-4} \text{ N}$$

8.1.3 Calculation of Equilibrium Falling Speed

Here, (5.5) is used as discussed in Chapter 5 to obtain the actual value of the falling speed.

$$L = \rho S v_z^2 \cdot (2a - 2a^2)$$

The axial induction factor, a , is the only fully empirical value that needs to be entered and was simulated to be 0.313 for an average maple seed. (**Holden 2015**)

Therefore, the equation can be solved using the other known variables.

$$\Leftrightarrow v_z = 0.888623 \text{ m/s}$$

This falling speed **deviates 5.47%** from the actual falling speed, which is a very good approximation given the limited amount of details that are known of the provided maple seed. A reasonable amount of deviation from the actual falling speed should be expected to leave room for a further increase of accuracy when this method is applied using more detailed measurements of variables such as known values for the geometrical parameters defined in Chapter 6, the actual function describing the chord length or the actual function describing the coefficient of lift.

8.1.4 Reiteration

Using this newly obtained value for the equilibrium falling speed, the calculation of lift ought to be redone.

$$L = 2.5556 \cdot 10^{-4} \text{ N}$$

Already, it can be concluded that the value of lift has only changed by a miniscule amount that is unlikely to cause drastic differences in the equilibrium falling velocity. However, to complete the calculation the falling speed is recalculated as follows.

$$v_z = 0.88972 \text{ m/s}$$

The resulting change is only 0.12% after performing the first and most important iteration. The conclusion is therefore made that although the constructed method has an inherent tendency towards an iterative solution, it is shown to be of negligible importance and can for the sake of simplicity be left asides or only performed once.

8.1.5 Falling Time Ratio

Since the fall duration is obviously dependent on the height from which the seed is released, an arbitrary value can be chosen. The Red Maple, one of the more common American species, grows to be, on average, 21.3 meters tall (**Jasey 2019**). Since the seed wouldn't fall from the top of the tree, an average release height of 20 meters is used for both calculation examples.

The fall duration in freefall can be calculated using (7.12), whereas the duration in air can be calculated using (7.14), the results are provided by Table 8.3.

Table 8.3 Fall durations of example seed one

$\Delta t_{freefall} \text{ (s)}$	$\Delta t_{air} \text{ (s)}$
2.02	23.02

Consequently, the research question can be answered for this example: the seed falls **11.4 times longer** in air than in freefall.

8.2 Example Two

A second maple seed from the same research paper, written by **Varshney 2011**, can be used to calculate and verify the falling speed during force equilibrium. The variables that are given are the same as for the previous maple seed, although with different values, given by Table 8.4.

Table 8.4 Known parameters of example seed two

m (mg)	S (mm ²)	ω (rad/s)	v_z (m/s)
195.8	546.1	82.7	1.18

When comparing these parameters to the previous example, the larger mass and smaller surface area can be hypothesized to speed up the resulting falling speed, this preliminary conclusion is observed in the measured falling speed; however, the question remains whether the constructed method can account for these variances in geometry to influence the calculated falling speed in a reasonable fashion.

8.2.1 Preliminary Falling Speed

The same general equation, (3.5), can be stated and filled in using the same logic as the previous calculation example. The values of the unknown variables can therefore be re-used, given by Table 8.5.

$$mg = \frac{1}{2} \rho S \left[\left(\frac{3}{4} \omega R_{tot} \right)^2 \cdot c_L + v_{z,preliminary}^2 c_D \right]$$

Table 8.5 Assumed values for the calculation of preliminary speed two

g (m/s ²)	ρ (kg/m ³)	c_L	c_D
9.81	1.225	1.0586	1.98

Using this information, the value of the preliminary falling speed can be computed.

$$v_{z,preliminary} = 1.17 \frac{\text{m}}{\text{s}}$$

Already, this value is shown to be surprisingly close to the actual falling speed. However, the possibility exists that this is purely luck due to the large amount of assumptions and simplifications used in this preliminary method of calculation.

8.2.2 Calculation of Lift

Using this preliminary value of falling velocity during force equilibrium, the general equation of lift, (4.5), can be restated and consequently solved.

$$L = \frac{1}{2} \rho \omega^2 \int_0^{B \cdot R_{tot}} R^2 \cdot c_L(R) \cdot c(R) dR$$

The calculation of the tip loss correction factor, B , uses the same logic applied to the previous calculation example and ought not to be reformulated. According to the empirical value of B calculated in Section 8.1.2, only 80.7% of the wing span of an average maple seed is effectively used for generating lift.

The same method and logic as elaborated in Section 8.1.2 were used and the value of lift has been computed using MATLAB.

$$L = \frac{1}{2} \rho \omega^2 \int_0^{B \cdot R_{tot}} R^2 \cdot c_L(R) \cdot c(R) dR$$

$$L = 4.3049 * 10^{-4} \text{ N}$$

8.2.3 Calculation of Equilibrium Falling Speed

(5.5) Is used as provided in Chapter 5 to obtain the actual value of the falling speed using the same, simulated value for the axial induction factor, a . (**Holden 2015**)

$$L = \rho S v_z^2 \cdot (2a - 2a^2)$$

The equation can be solved using the other known variables.

$$\Leftrightarrow v_z = 1.22 \text{ m/s}$$

This falling speed **deviates 3.66%** from the actual falling speed. Which produces an average percentual error of 4.57% for the calculation of the falling speed. Considering the amount of uncertainty given by the limited known variables, the constructed method has proven itself remarkably accurate for these two example calculations. The distinct difference in geometry and consequent falling speed is clearly accounted for in the end results of falling speeds, which is a feat that previous research has been unable to include in such a straight forward and simple manner as provided by this paper.

8.2.4 Falling Time Ratio

Using the same arbitrary height as referenced in Section 8.1.5, the falling time ratio can be calculated.

The fall duration in freefall can be calculated using (7.12), whereas the duration in air can be calculated using (7.14). The results are provided by Table 8.6.

Table 8.6 Fall durations of example seed two

$\Delta t_{freefall}$ (s)	Δt_{air} (s)
2.02	17.01

Consequently, the research question can be answered for this example: the seed falls **8.42 times longer** in air than in freefall. The discrepancy with the previously calculated falling time ratio from Section 8.1.5 makes sense: one could presume that a heavier and smaller seed will fall more quickly and therefore differ less from duration it would take to fall in freefall.

9 Conclusions

The paper has constructed and validated a method describing the aerodynamics of a maple seed and allowing the calculation of its equilibrium falling speed and consequent ratio comparing the fall duration in air to in freefall. An effort has been made to provide ample flexibility in including variances in maple seed geometry to account for a large biodiversity in the available seeds. The method aims to be primarily fundamentally based and would be considered to have succeeded in that aspect although some variables are still required to be substituted with empirical values. The validation of this paper as is shown in the example calculations has proven to be sufficiently accurate given the relatively small amount of data that is known about the calculation examples. The three-step method of calculating the falling speed provided by this paper proves to be a simpler alternative when compared to preceding computational methods in this field of research. A lack of validation of these alternative methods of calculation such as unsteady BEM theory refrains the possibility of an exact comparison between previously stated methods and the method given by this paper.

The essential calculation of lift performed in this paper provides the possibility to incorporate an extensive amount of specifications of a maple seed and derives its main advantage from that flexibility combined with its ease of use. Other developed frameworks describing the respective aerodynamics have failed to allow the incorporation of such intricate details of geometry, such as chord length and twist, that are essential for an accurate calculation of the falling time. Especially when considering and comparing individual differences of maple seeds with distinct geometries, the provided method proves to be reliable and accurate.

An important conclusion confirming visual evidence of falling maple seeds is that of the large angles of attack that occur when considering the small rotational velocity found in maple seeds. These large angles of attack require the maple seed to derive its lift using solely post-stall angles of attack. As stated in Subchapter 4.3, the evolutionary pressure to opt for post-stall angles instead of conventional angles of attack is the most beneficial option for achieving the largest amount of lift.

The final calculation of falling speed as discussed in Chapter 5 uses Blade Element Momentum Theory and consequently adopts many of its assumptions and inaccuracies. Moreover, the power coefficient that is used stems from a simulation of a maple seed and is immutable with respect to variances in geometry. However, BEMT is used only to a relatively small extent and a more fundamentally based method of calculating falling speed from lift can be a task for future research. The assumption is made that the coefficient of power is the parameter that is evolutionarily optimized, altering geometry to sustain this variable in the process. Even though such assumptions have been made, example calculations have proven to be remarkably accurate therefore rendering these assumptions either true or of minor influence.

The calculation of a falling time or fallen distance as a function of time is devalued due to a lack of experimental data which can be used to validate any constructed method of approximating the behavior of a falling maple seed while in transitional period. The constructed model describing fallen distance with respect to time is therefore yet to be validated and can until validation only be assumed to be an approximation based solely on logical reasoning. However, when accounting for the possibility of a flaw due to assumption it can be stated that as based on two calculation examples a maple seed falls 9.91 times longer when in air when compared to freefall.

10 Recommendations

As previously stated, the most significant limitation in completing this theoretical framework lies in the lack of more validation, needed to provide reliability and value to the constructed aerodynamical and mechanical models. Most importantly, measurements of the falling time of maple seeds when released from a certain height would aid this research in providing either support for or disapproval of the constructed framework. Secondly, an addition of more calculation examples for validation of the equilibrium falling speed, stemming from multiple sources, would largely benefit the validation of the method in general.

In order to divert the method into an even more fundamentally based one, several empirical values could be investigated whether a relationship to the known parameters such as geometrical features and weight can be formed. Such currently empirical values include the angular velocity, ω , and the axial induction factor, a .

Lastly, the unconventional progression of twist along the wingspan of the maple seed that has been found in Subchapter 4.3 is yet to be fundamentally discussed and explained.

List of References

- Airfoil Tools 2019** AIRFOIL TOOLS: Calculated polar for: NACA 2408, 2019. – Available at: <http://airfoiltools.com/airfoil/details?airfoil=naca2408-il>, archived as: <https://perma.cc/H3S3-ETUF>
- Caley 2013** CALEY, Thomas; HOLDEN, Jake; TURNER, Mark: *Flow Simulation of a Maple Seed*. Cincinnati : University of Cincinnati, 2013. – Available at: https://www.academia.edu/32427521/Maple_Seed_Performance_as_a_Wind_Turbine, archived as: <https://perma.cc/S3WM-6GUX>
- Ehrich 2018** EHRICH, Sebastian; SCHWARZ, Carl Michael; RAHIMI, Hamid; STOEVE SANDT, Bernhard; PEINKE, Joachim. Comparison of the Blade Element Momentum Theory with Computational Fluid Dynamics for Wind Turbine Simulations in Turbulent Inflow. *Journal of Applied Sciences*, vol. 8, no. 12, 2018. - URL: <https://doi.org/10.3390/app8122513>
- Frénot 1960** FRÉNOT, G. H.; HOLLOWAY, Arthur Herbert: *Agard Aeronautical Multilingual Dictionary*. Oxford : Pergamon Press, 1960. - URL: <https://doi.org/10.1017/S0001924000093660>
- Hinz 2014** HINZ, Juliane: *Maple Seed*. Tübingen : Eberhard Karls Universität Tübingen, 2014. – Available from: <https://archive.org/details/MapleSeed>
- Holden 2015** HOLDEN, Jacob R.; CALEY, Thomas M.; TURNER, Mark G.: *Maple Seed Performance as a Wind Turbine*. Cincinnati : University of Cincinnati, 2015. – URL: <https://doi.org/10.2514/6.2015-1304>
- Jasey 2019** JASEY, Kelley: *What Is the Average Height of Adult Maple Trees*, 2019. Available at: <https://homeguides.sfgate.com/average-height-adult-maple-trees-41440.html>, archived as: <https://archive.org/details/WhatIsTheAverageHeightOfAdultMapleTreesHomeGuidesSFGate>
- Kulunk 2011** KULUNK, Emrah: *Aerodynamics of Wind Turbines, Fundamental and Advanced Topics in Wind Power*. New Mexico : New Mexico Institute of Mining and Technology, 2011. – URL: <https://doi.org/10.5772/17854>

- Lee 2017** LEE, Injae; CHOI, Haecheon: *Flight of a falling maple seed*. Seoul : American Physical Society, 2017. – URL: <https://doi.org/10.1103/PhysRevFluids.2.090511>
- Matič 2015** MATIČ, Gašper; TOPIC, Marko; JANKOVEC, Marko: Mathematical Model of a Monocopter Based on Unsteady Blade-Element Momentum Theory. *Journal of Aircraft*, vol. 41, no. 6, 2015. – URL: <https://doi.org/10.2514/1.C033098>
- Oxford 2019** OXFORD ENGLISH DICTIONARY (OED). Oxford University Press, 2019. – URL: <https://en.oxforddictionaries.com>
- Petrilli 2013** PETRILLI, Justin; PAUL, Ryan; GOPALARATHNAM, Ashok; FRINK, Neal T: *A CFD Database for Airfoils and Wings at Post-Stall Angles of Attack*. Hampton, Virginia : NASA Langley Research Center, 2013. – URL: <https://doi.org/10.2514/6.2013-2916>
- Sovran 1978** SOVRAN, Gino; MOREL, Thomas; MASON, William T. Jr.: *Aerodynamic drag mechanisms of bluff bodies and road vehicles*. New York : Plenum Press, 1978 – URL: <https://doi.org/10.1007/978-1-4684-8434-2>
- Varshney 2011** VARSHNEY, Kapil; CHANG, Song; WANG, Jane Z: *The kinematics of falling maple seeds and the initial transition to a helical motion*. Ithaca, USA : Cornell University, 2011. – URL: <https://doi.org/10.1088/0951-7715/25/1/C1>

All references have been consulted on 2019-06-01.